First Regge parameterisation of polarized DIS cross section.

E. Thomas * and N. Bianchi
INFN-Laboratori Nazionali di Frascati, CP 13, I-00044 Frascati, Italy

The first Regge description of the virtual photon absorption cross section difference $\Delta\sigma(\gamma^*, N) = \left[\sigma_{1/2}(\gamma^*, N) - \sigma_{3/2}(\gamma^*, N)\right]$ was obtained from a global fit of all the data collected by the experiments measuring spin asymmetries in polarized lepton - polarized nucleon deep inelastic scattering. This work present a phenomenological and a numerical description of all the polarized deep inelastic data ($\Delta\sigma(\gamma^*, N)$, g_1 spin structure function) on the whole measured kinematical range (0.3 GeV$^2 < Q^2 < 70$ GeV^2, 4 GeV$^2 < W^2 < 300$ GeV^2). The fit also provide reliable predictions for the photo-production limit through a smooth Q^2-transition.

1. Introduction

A fundamental sum rule relating the cross section difference $\Delta\sigma = [\sigma_{1/2} - \sigma_{3/2}]$, where $\sigma_{1/2}$ and $\sigma_{3/2}$ are the real photon-nucleon absorption cross section of total helicity 1/2 and 3/2 respectively, to the anomalous contribution κ to the magnetic moment of the nucleon as been derivated by Gerasimov, Drell and Hearn[1] (GDH):

$$I = \int_0^\infty \Delta\sigma(\nu)\frac{d\nu}{\nu} = -\frac{2\pi^2\alpha}{m^2}\kappa^2, \quad (1)$$

where ν is the photon energy. This sum rule as never been tested directly. Experiments [2] are planned to measure $\Delta\sigma(\nu)$ up to $\nu = 3$ GeV. Multipole analysis of single pion photo-production amplitudes and estimates of the double pion contribution from the nucleon resonance decays provided an indication of the low energy contribution to the sum rule [3] [4], which is expected to be the dominant one. All these findings strongly disagree with the sum rule expectations.

However, the high energy contribution to the GDH sum rule is missing in all the estimates and will not be accessible to the foreseen experiments. For the moment, only a $Q^2 = 0$ extrapolation of $\Delta\sigma(\nu, Q^2)$, accessible through polarised deep-inelastic-scattering (DIS) experiments, can provide an estimate of the non resonance contribution to GDH sum rule.

*This work was partially supported by the TMR contribution (contract FMRX-CT96-0008) from the European Community.

The spin asymmetries measured in inclusive deep-inelastic-scattering of polarised leptons off polarised nucleons can be interpreted in term of target nucleon parton spin distributions. NLO-QCD fits [5] already provide a good description of this process. However, these parameterisations cannot be extrapolated unambiguously to the real photon case.

For the total *unpolarised* photon nucleon absorption cross section, it as been pointed out [6] that Regge language can provide a similar description for real and virtual photon, taking into account the threshold effect arising from the virtual particle exchange. Regge fit of the total $\gamma^* p$ cross section from highest Q^2 available experimentally to $Q^2 = 0$ through smooth Q^2 transition was successfully performed [7].

In this work, a similar approach was applied to *polarised* DIS data : the measured spin asymmetries were first converted in cross section differences, $\Delta\sigma(\nu, Q^2)$, simply by multiplying them by the total cross section. These cross section differences were fitted with a Regge parameterisation with a smooth phenomenological Q^2 dependence.

2. Regge phenomenology

The Regge theory provided a good description of the high-energy behavior of the cross sections for a large number of processes[8]. In this framework the cross section behaviors are given by $\sigma \sim s^{\alpha^0 - 1}$ where s is the center of mass square energy and α^0 is the intercept of the leading Regge trajectory for the given process. The intercept

$\alpha^0 = J - \alpha' m_t^2$ is determined by the spin J and mass m_t of the exchanged particle and by the trajectory slope $\alpha' \simeq$ 0.8-0.9 GeV^{-2}. In the case of the absorption of circularly polarised photons on polarised nucleon it is useful to consider the isovector and the isoscalar terms of the interaction[9].

The isovector contribution to $\Delta\sigma$ is described by the $a_1(1260)$ meson trajectory : $\Delta\sigma_V \sim s^{\alpha^0_{a1}-1}$. The axial vector meson a_1 is still now an elusive prey in most of experiments due to its large width and the presence of strong background. Experiments of the last twenty years provided contradictory measurements of the a_1 meson mass and width over the wide ranges 1.05-1.28 GeV and 0.24-0.61 GeV, respectively[10]. The expected value of the a_1 meson intercept is about -0.3, but due to the uncertainties in the knowledge of the mass and of the trajectory slope, a possible range between 0 and -0.5 is generally considered.

The isoscalar contribution to $\Delta\sigma$ is described by the $f_1(1285)$ meson trajectory $\Delta\sigma_I \sim s^{\alpha^0_{f1}-1}$. Being the f_1 meson mass well known, its intercept is expected to be about -0.4 ± 0.1. In addition it has been shown that the exchange of two non-perturbative gluons can provide an isoscalar contribution $\Delta\sigma_I \sim (1/s)ln(s/\mu^2)$ where the mass parameter μ has the typical hadronic scale $\mu \sim 1$ GeV[11].

In this work we consider the above described contributions for the case of photo-absorption of circularly polarised virtual photon on polarised nucleon where the centre of mass square energy is given by $W^2 = m^2 + 2m\nu - Q^2$.

3. Data analysis and fitting procedure

We have analyzed the data from deep inelastic scattering of longitudinally polarised leptons off polarised ^{1}H, ^{2}H and ^{3}He targets which provided measurements of the photo-absorption asymmetry A_1 for the proton, deuteron and neutron respectively. The measurements were performed by six experiments at CERN (EMC[12], SMC[13]), SLAC (E142[14], E143[15], E154[16]) and DESY (HERMES[17]). For each experiment we considered the data set with the most detailed Q^2 and x binnings. Therefore we did not include in the fit the Q^2-averaged data which are generally used for the determination of the polarised structure function $g_1(x)$. A total of 511 independent data points was included in the analysis: specifically 238 proton data, 81 neutron data and 192 deuteron data. The kinematic range covered by the data is 0.3 GeV^2 $< Q^2 <$ 70 GeV^2 and 4 GeV^2 $< W^2 <$ 300 GeV^2 for the proton and deuteron, and 1 GeV^2 $< Q^2 <$ 15 GeV^2 and 4 GeV^2 $< W^2 <$ 70 GeV^2 for the neutron.

The cross section difference $\Delta\sigma$ was derived from the measured virtual photo-absorption asymmetry A_1 and from the unpolarised structure function F_1:

$$\Delta\sigma = 2A_1\sigma_T = \frac{8\pi^2\alpha}{m}\,\frac{A_1F_1}{K}, \qquad (2)$$

where σ_T is the total transverse cross section and $K = \sqrt{\nu^2 + Q^2}$ is the virtual photon flux factor. The structure function $F_1 = F_2(1+\gamma^2)/(2x(1+R))$ was calculated from published parameterisations of the unpolarised structure functions F_2 [18] for the proton, neutron and deuteron and of $R = \sigma_L/\sigma_T$, the ratio of the absorption cross sections [19] for longitudinally and transversely polarised virtual photons. The structure function R was assumed to be independent of the target ($R^p = R^n = R^d$).

The $\Delta\sigma$ experimental data were reproduced by a global 3-D fit over the Q^2 and W^2 variables and the isospin dimension T:

$$\Delta\sigma = \Delta\sigma(T, W^2, Q^2) = \left[2aW^{2(\alpha^0_{a1}-1)}T + fW^{2(\alpha^0_{f1}-1)} + g\frac{lnW^2}{W^2}\right]F, \qquad (3)$$

where F is the threshold factor

$$F = \left[\frac{W^2 - W_\pi^2}{W^2 - W_\pi^2 + Q^2 + m_r^2}\right]^p, \qquad (4)$$

where $W_\pi = 1.07$ GeV is the single pion electroproduction threshold and $m_r = 1.26$ GeV is a common mass scale of the exchanged particles which is close to the a_1 and f_1 meson masses and to the two gluon exchange hadronic scale. The exponent p is given by

$$p = 1.5 \left(1 + \frac{Q^2}{Q^2 + M^2}\right), \tag{5}$$

being M a free parameter of the fit. This threshold factor is similar to the ones used in the description of unpolarised cross section σ_T accounting for the behavior of a cross section corresponding to a virtual particle with $W^2 > Q^2$ [6] [7] [20] [21]. F increases from 0 at the pion electroproduction threshold to ≈ 1 at high W^2, when $W^2 \gg Q^2$.

Because Regge theory gives no indication about the relative weight and Q^2-dependence of the various contributions, the three coefficients in eq. 3 were parametrised with a simple and smooth Q^2-dependence, with two free parameters each :

$$a, f, g = p_1^{a,f,g} + p_2^{a,f,g} t, \tag{6}$$

where

$$t = log \frac{log \frac{Q^2 + Q_0^2}{\Lambda^2}}{log \frac{Q_0^2}{\Lambda^2}}. \tag{7}$$

Here Λ and Q_0^2 are the QCD cutoff and scale parameters, respectively. We used $\Lambda = 0.255$ GeV and $Q_0^2 = 0.278$ GeV^2 in agreement with the ALLM parameterisation for the unpolarised total transverse cross section σ_T[7].

The cross section difference for the proton and neutron were defined by eq. 5 with T=+1/2 and T=−1/2, respectively. The cross section difference for the deuteron was defined $\Delta\sigma^d = [\Delta\sigma^p + \Delta\sigma^n](1 - 1.5\omega_D)$ where $\omega_D = 0.05$ is the D-wave probability in the deuteron[22].

4. Results

In the following we describe three different models we used to reproduce the $\Delta\sigma$ data. The results of the three models are presented in Table 1.

Model I

We fitted proton, neutron and deuteron data using the parameterisation described in the previous section and with 9 free parameters $(\alpha^0_{a1}, \alpha^0_{f1}, p^a_1, p^a_2, p^f_1, p^f_2, p^g_1, p^g_2, M^2)$. The fit reproduced the data with reduced $\chi^2/ndf = 1.14$. The intercept of the f_1-meson trajectory was found within the expected range. On the contrary, the intercept of the a_1-meson trajectory was not consistent with the standard Regge theory. This finding may imply that the a_1-meson trajectory is strongly not linear or not parallel to the other meson trajectories (like the a_2-meson or the ρ-meson ones).

Table 1
Parameter values provided by the fit of the data with the different models. The error estimates have been obtained from a MINOS analysis of the MINUIT program.

	Model I	Model II	Model III
p_1^a [μb]	107±6	133±4	45 ±27
p_2^a [μb]	-40±4	-75±3	107 ±47
p_1^f [μb]	83±25	112±21	119±15
p_2^f [μb]	141±47	64±24	51±17
p_1^g [μb]	-22±3	-28±3	-34±2
p_2^g [μb]	20±2	23±2	24±2
p_1^r [μb]	-	-	36±2
p_2^r [μb]	-	-	-19±1
M^2 [GeV^2]	3.7±0.7	4.8±0.8	2.9±0.5
$\alpha^0_{a_1}$	0.17±0.02	$(0.21 \pm 0.02) \cdot t$	-0.44±0.13
$\alpha^0_{f_1}$	-0.44±0.09	-0.32±0.09	-0.23±0.05
α^0_r	-	-	0.46±0.02
χ^2/ndf	1.14	1.12	1.13

Model II

To cure the problem of non-linearity or non-parallelism of the previous model we introduced in the fit a smooth Q^2-dependence of a_1-meson intercept assuming it equal to 0 for Q^2=0 and varying linearly with t. With this assumption, the errors of the parameters of the coefficients and the χ^2/ndf were decreased. The intercept of the f_1-meson trajectory was found in excellent agreement with the expectation. The intercept of the a_1-meson trajectory changed of 0.25 in the Q^2 range 0-10 GeV^2. This behavior is similar to the Q^2-evolution of the reggeon and the pomeron intercepts found in the description of the unpolarised σ_T data[7].

Model III

In this parameterisation, we considered an additional reggeon trajectory $2rW^{2(\alpha_r^0-1)}T$ for the isovector part of the interaction, with no Q^2-dependence of the intercepts. The result of this Model are only slightly worse respect to the ones of Model II. The intercept of the f_1-meson trajectory is within the expectation range. The intercept of the a_1-meson trajectory was found in agreement with the expectation. The intercept α_r^0 of the additional reggeon trajectory was found close to the a_2-meson intercept ≈ 0.5.

The comparison between the results of the three models and the experimental data as function of the three variables (T, W^2 and Q^2) is shown in fig. 1. For this purpose the data are presented grouped in Q^2-bins. All the three Models provide a rather good description of the present data. In the following, we show the results for the Model II which provide the best χ^2/ndf and which has the simplest phenomenological interpretation for the isovector component.

In fig. 2 are also shown the results of Model II for Q^2=0. The expectations for real photons are: $\Delta\sigma^p$ is positive, ranging between 0 and $\sim 23\mu$b; $\Delta\sigma^n$ is negative and ranges between ~ -14 and 0μb; $\Delta\sigma^d$ ranges between $+12$ and -4μb being positive below $\nu \sim 3.5$ GeV. These predictions are confirmed by the recent E155 [23] measurement of inclusive hadron photoproduction asymmetry, which clearly show that $\Delta\sigma^p$ is positive and that $\Delta\sigma^n$ is negative. These large cross sections show that the non resonance contribution to the GDH sum rule is significant, and is even the dominant contribution to the isovector channel. If one take into account the non resonance contribution predicted by these models, the GDH sum rule is fullfiled [24].

A further comparison between Model II and experimental data is provided in fig. 3 where the expectations for the polarised structure functions $g_1(x)$ are shown. These were evaluated at $Q^2 = 3$ GeV^2 using eqs. 2 and 3 for model II under the approximation that $g_1(x,Q^2) \approx A_1(x)F_1(x,Q^2)$. The curves are compared with $g_1(x)$ Q^2-averaged data evolved at the same Q^2 and with a NLO-QCD fit based on polarised parton density distributions[5]. Our Model and the QCD model are in good agreement at least for $x \geq 0.03$ and both well reproduce the experimental data. At low-x, where they are different, the present experimental uncertainties are too large to provide strong constraints for both models. Measurements of the spin structure functions at very low-x using the HERA polarised collider[25] will shed light on this subject. Also shown in fig. 3 are the a_1-meson, f_1-meson and two-gluons exchange individual contributions. In this framework, the stronger experimental variation of g_1^n at low-x respect to g_1^p is simply explained by the similar low-x behaviors of the isovector and the isoscalar components in the neutron. The change of sign of g_1^d is at $x \approx 0.015$ and is due to the different x-dependence of the two isoscalar components, being the f_1-meson positive contribution dominating at large-x, while the two-gluons negative one at low-x.

The very recent E155 [26] g_1^d data displayed in fig. 3 were not included in the fit. These data seems to support a change of sign in the g_1^d structure function around $x \approx 0.02$. If this change of sign if confirmed, it means that the minimal Regge model aiming to describe polarised photon-nucleon absorption cross section should have at least two isoscalar components, and of course one isovector component to match the very different g_1^p and g_1^n behavior.

5. Conclusions

We have studied the deep inelastic scattering of longitudinally polarised leptons off polarised targets in terms of polarised cross sections. The cross sections have been fitted by three different parameterisations in which the isovector and the isoscalar contributions from Regge inspired models have been considered.

With these parameterisations we were able to well describe, over the whole kinematic range of Q^2 and W^2, the experimental polarised cross sections $\sigma_{1/2} - \sigma_{3/2}$ and structure functions g_1 for the proton, neutron and deuteron.

Our models also provide reliable estimates for the real photon case, showing a significant non

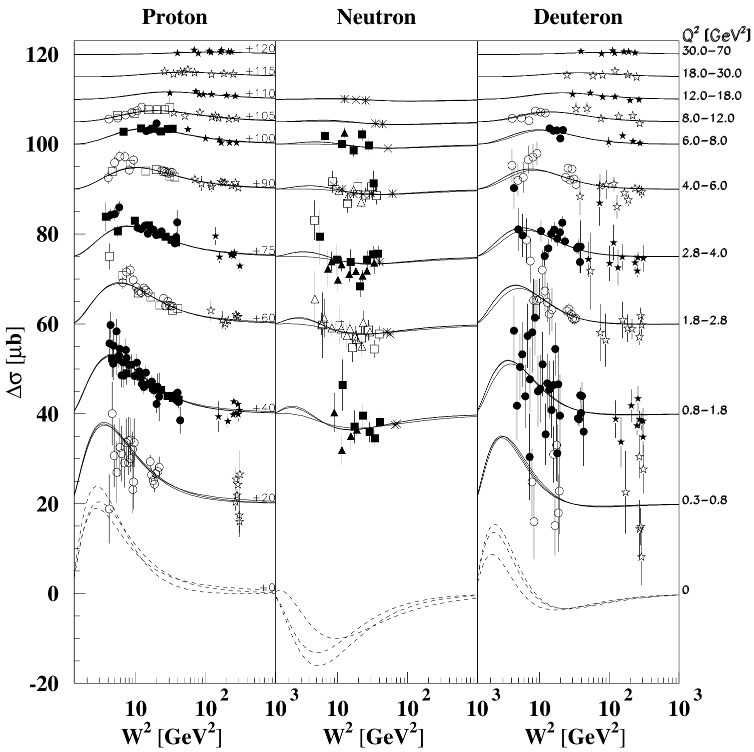

Figure 1. Cross section differences as a function of W^2 for different Q^2-bins (on the right scale). Data are from Refs. [12,13] (stars), [14] (triangles), [15] (circles), [16] (asterisks), and [17] (squares). For a better view, a Q^2-increasing constant value (on the right side of the proton panel) has been added to the data which are presented with open and close symbols alternatively. Only data with statistical error lower than 10 μb are shown. The solid curves are the results of the three models calculated for the average Q^2-values in each Q^2-bin. The dashed curves are the models predictions for Q^2=0.

resonance contribution to GDH sum rule.

REFERENCES

1. S.B. Gerasimov, Sov. J. Nucl. Phys. **2** (1966) 430; S.D. Drell and A.C. Hearn, Phys. Rev. Lett. **16** (1966) 908.
2. N. Bianchi, Proc. Workshop on Electron Nucleus Scattering, O. Benhar and A. Fabrocini editors, Elba, July 1-5, 1996, p.363 and references therein.
3. I. Karliner, Phys. Rev. **D 7** (1973) 2717.
4. D. Drechsel and G.Krein, Phys. Rev. **D 58** (1998) 116009.
5. M. Gluck, E. Reya, M. Stratmann and W. Vogelsang, Phys. Rev. **D 53** (1996) 4775.
6. A. Levy and U. Maor, Phys. Lett. **B 182** (1986) 108.
7. H. Abramowicz, E.M. Levin, A. Levy and U. Maor, Phys. Lett. **B 269** (1991) 465.
8. A. Donnachie and P.V. Landshoff, Phys. Lett. **B 296** (1992) 227.
9. R.L. Heimann, Nucl. Phys. **B 64** (1973) 429.
10. Particle Data Group, Phys. Rev. **D 54** (1996) 1.
11. S.D. Bass and P.V. Landshoff, Phys. Lett. **B**

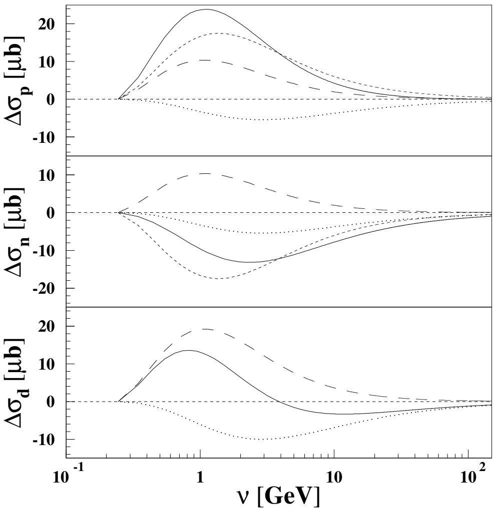

Figure 2. Model II predictions for real photons: the short-dashed, long-dashed and dotted curves are the a_1, f_1 and two-gluons contributions respectively. The solid curves are the sum of the different contributions.

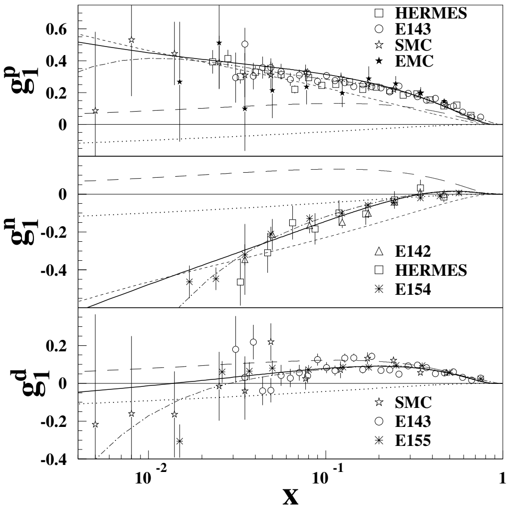

Figure 3. Spin structure functions $g_1(x)$ at $Q^2 = 3$ GeV^2 (same notation as Fig. 1, for the data). The solid curves are the results of Model II. The short-dashed, long-dashed and dotted curves are the a_1, f_1 and two-gluons contributions respectively. The predictions of a NLO-QCD fit [5] are indicated by the dot-dashed curves. The very recent E155 data for the deuteron were not included in the fit.

336 (1994) 537.
12. EMC Collaboration, J. Ashman *et al.*, Nucl. Phys. **B 328** (1989) 1.
13. SMC Collaboration, B. Adeva *et al.*, Phys. Rev. **D 58** (1998) 112001.
14. E142 Collaboration, P.L. Anthony *et al.*, Phys. Rev. **D 54** (1997) 6620.
15. E143 Collaboration, K. Abe *et al.*, Phys. Rev. **D 58** (1998) 112003.
16. E154 Collaboration, K. Abe *et al.*, Phys. Rev. Lett. **79** (1997) 26.
17. HERMES Collaboration, K. Ackerstaff *et al.*, Phys. Lett. **B 444** (1998) 531; K. Ackerstaff *et al.*, Phys. Lett. **B 404** (1997) 383; A. Airapetian *et al.*, Phys. Lett. **B 442** (1998) 484.
18. NMC Collaboration, M. Arneodo *et al.*, Phys. Lett. **B 364** (1995) 107.
19. L.W. Whitlow *et al.*, Phys. Lett. **B 250** (1990) 193.
20. A. Capella, A. Kaidalov, C. Merino and J. Tran Thanh Van, Phys. Lett. **B 337** (1994) 358.
21. P. Desgrolard, L. Jenkovszky and F. Paccanoni, hep-ex 9803286, to be published in Eur. Phys. J. **C**.
22. R. Machleidt *et al.*, Phys. Rep. **149** (1987) 1.
23. E155 Collaboration (P.L. Anthony et al.). SLAC-PUB-8049, Feb 1999.
24. N. Bianchi and E. Thomas, Phys. Lett. **B 450** (1999) 439.
25. A. De Roeck *et al.*, Eur. Phys. J. **C 6** (1999) 121.
26. E155 Collaboration (P.L. Anthony et al.). SLAC-PUB-8041, Mar 1999.